

THREE-DIMENSIONAL ANALYSIS OF FREQUENCY-CHIRPED FELS

Z. Huang, Y. Ding, J. Wu

SLAC National Accelerator Laboratory, Menlo Park, CA 94025, USA

Abstract

Frequency-chirped free-electron lasers (FELs) are useful to generate a large photon bandwidth or a shorter x-ray pulse duration. In this paper, we present a three-dimensional analysis of a high-gain FEL driven by the energy-chirped electron beam. We show that the FEL eigenmode equation is the same for a frequency-chirped FEL as for an undulator-tapered FEL. We study the transverse effects of such FELs including mode properties and transverse coherence.

INTRODUCTION

Frequency-chirped free-electron lasers (FELs) can be produced by an energy-chirped electron beam and can provide a relatively large bandwidth for x-ray applications and manipulations. One-dimensional theory of frequency-chirped FELs have been developed in Refs. [1–3]. In this paper, we present a three-dimensional analysis of frequency-chirped FELs, focusing on the case of self-amplified spontaneous emission (SASE). We study the transverse effects including mode properties and transverse coherence and discuss possible applications to short-wavelength FELs.

FREQUENCY CHIRP AND UNDULATOR TAPER

In this section, we show analytically the equivalent effect on the FEL gain between frequency chirp and undulator taper, first discussed in Ref. [2] through simulation studies. We assume a parallel electron beam without emittance and start with the FEL pendulum equation

$$\frac{d\theta}{d\bar{z}} = \bar{\eta}, \quad \frac{d\bar{\eta}}{d\bar{z}} = ae^{i\theta} + \text{c. c.}, \quad (1)$$

where $\theta = (k_r + k_u)z - \omega_r t$ is the electron phase variable, $\lambda_u = 2\pi/k_u$ is the undulator period, $\lambda_r = \lambda_u(1 + K^2/2)/(2\gamma_0^2) = 2\pi/k_r = 2\pi c/\omega_r$ is the resonant wavelength, γ_0 is the average beam energy in units of mc^2 , K is the undulator parameter, $\bar{z} = 2k_u \rho z$, $\bar{\eta} = (\gamma - \gamma_r)/(\gamma_0 \rho)$ is the scaled energy variable, ρ is the FEL parameter [5], $a(\bar{\mathbf{x}}, \theta; \bar{z})$ is the scaled (complex) field amplitude, and c. c. stands for complex conjugate. We consider an electron beam with a linear energy chirp given by

$$h = -\frac{d\gamma/\gamma_0}{dt} \frac{1}{2\rho^2\omega_r}. \quad (2)$$

Note that the scaled chirp parameter is defined as the relative energy change (normalized by ρ) over a cooperation length $\lambda_r/(4\pi\rho)$. For a positive chirp, the head of the bunch has a higher energy than the tail.

The linearized Vlasov equation for the electron distribution function is

$$\frac{\partial f_1}{\partial \bar{z}} + \bar{\eta} \frac{\partial f_1}{\partial \theta} + (ae^{i\theta} + \text{c. c.}) \frac{\partial f_0}{\partial \bar{\eta}} = 0, \quad (3)$$

where f_1 is the perturbed distribution function describing the FEL microbunching, $f_0 = U(\bar{\mathbf{x}})\delta(\bar{\eta} - h2\rho\theta)$ is the average distribution function, δ is the Dirac delta function for a beam with a vanishing slice energy spread, $U(\bar{\mathbf{x}})$ is the transverse profile of the electron beam with the normalization $U(0) = 1$, and $\bar{\mathbf{x}} = \sqrt{2k_u k_r}(x, y)$ represents the (scaled) transverse coordinates. The solution of the Vlasov equation is

$$f_1(\theta, \bar{\eta}; \bar{z}) = f_1(\theta, \bar{\eta}; 0) - \int_0^{\bar{z}} d\bar{s} \left[a(\bar{s})e^{i[\theta + \bar{\eta}(\bar{s} - \bar{z})]} + \text{c. c.} \right] \frac{\partial f_0}{\partial \bar{\eta}}. \quad (4)$$

The Maxwell equation under the slowly varying amplitude and phase approximation is

$$\begin{aligned} \left(\frac{\partial}{\partial \bar{z}} + \frac{\partial}{2\rho\partial\theta} + \frac{\nabla_{\perp}^2}{2i} \right) a &= -e^{-i\theta} \int f_1(\theta, \bar{\eta}; \bar{z}) d\bar{\eta} \\ &= -e^{-i\theta} \int f_1(\theta, \bar{\eta}; 0) d\bar{\eta} + iU(\bar{\mathbf{x}}) \\ &\quad \times \int_0^{\bar{z}} d\bar{s} (\bar{z} - \bar{s}) a(\bar{s}) e^{ih2\rho\theta(\bar{s} - \bar{z})}, \end{aligned} \quad (5)$$

where $\nabla_{\perp}^2 = \partial^2/\partial\bar{\mathbf{x}}^2$. The first term of the last expression corresponds to shot noise modulations that start the FEL process (or any other modulations near the resonant wavelength imprinted on the beam). Let us drop this term for now and focus on the second term that gives rise to the exponential growth. We introduce a new field variable

$$\tilde{a}(\bar{\mathbf{x}}, \theta; \bar{z}) = a(\bar{\mathbf{x}}, \theta; \bar{z}) \exp [ih(2\rho\theta\bar{z} - 2\rho^2\theta^2)] \quad (6)$$

and insert into Eq. (5) to obtain

$$\begin{aligned} \left(\frac{\partial}{\partial \bar{z}} + \frac{\partial}{2\rho\partial\theta} + \frac{\nabla_{\perp}^2}{2i} \right) \tilde{a} &= iU(\bar{\mathbf{x}}) \int_0^{\bar{z}} d\bar{s} (\bar{z} - \bar{s}) \tilde{a}(\bar{s}) \\ &\quad + ih\bar{z}\tilde{a}(\bar{z}). \end{aligned} \quad (7)$$

Let us take Fourier transformation of the electric field

$$\tilde{a}(\bar{\mathbf{x}}, \theta; \bar{z}) = \int d\nu \tilde{a}_{\nu}(\bar{\mathbf{x}}; \bar{z}) e^{i\nu\theta}. \quad (8)$$

The field equation in the frequency domain is

$$\left[\frac{\partial}{\partial \bar{z}} + i\hat{\nu} + \frac{\nabla_{\perp}^2}{2i} \right] \tilde{a}_{\nu} = iU(\bar{\mathbf{x}}) \int_0^{\bar{z}} d\bar{s}(\bar{z} - \bar{s}) \tilde{a}_{\nu}(\bar{s}), \quad (9)$$

where $\hat{\nu} = \bar{\nu} - h\bar{z}$, and $\bar{\nu} = \nu/(2\rho) = (\omega - \omega_r)/(2\rho\omega_r)$ is the scaled detune parameter.

Following the treatment of undulator taper in Ref. [4] (especially Appendix B), one can show that the field equation for the undulator taper is the same as Eq. (9), except that $\hat{\nu} = \bar{\nu} - u\bar{z}$. Here $u = -KdK/dz(2\rho^2 k_u(2 + K^2))$ is the rate of the undulator taper. In presence of both frequency chirp and undulator taper, one can then arrange $h = -u$ to cancel these two terms in the field equation. Thus, the effects on the FEL gain from a chirped beam can be compensated by tapering the undulator properly, as pointed out in Ref. [2].

For $|h| < 1$, the field equation can be studied through the WKB approximation [4]. The solution can be written in the form

$$\tilde{a}_{\nu}(\bar{\mathbf{x}}; \bar{z}) \approx A(\bar{\mathbf{x}}; \bar{z}) \exp \left[-i \int_0^{\bar{z}} (\mu_0(\tau) + \mu_1(\tau)) d\tau \right], \quad (10)$$

where μ_0 is the zeroth-order growth rate, and μ_1 is the first-order correction to the growth rate that can have a significant contribution to the final power level. The FEL mode equation for the zeroth-order solution is

$$\left[\mu_0 - \hat{\nu} + \frac{\nabla_{\perp}^2}{2} \right] A(\bar{\mathbf{x}}; \bar{z}) = \frac{1}{\mu_0^2} A(\bar{\mathbf{x}}; \bar{z}) U(\bar{\mathbf{x}}), \quad (11)$$

Here $\hat{\nu} = \bar{\nu} - h\bar{z}$ is a \bar{z} -dependent frequency detune because of the energy chirp. Thus, the main effect of frequency chirp on the transverse mode is through the frequency detune. In what follows, we develop a simplified solution to the FEL mode equation and study the transverse effects introduced by frequency chirp (and undulator taper).

A SIMPLIFIED SOLUTION TO THE MODE EQUATION

For a Gaussian transverse profile of the electron beam, the FEL mode equation can be solved numerically using the matrix formulation [6]. In the x-ray region where the diffraction effect is small, the radiation mode size is typically narrower than the electron beam size. Assume equal rms beam size $\sigma_x = \sigma_y$, we can expand

$$U(\bar{\mathbf{x}}) = U(r) = \exp \left(-\frac{r^2}{2\bar{\sigma}_x^2} \right) \approx 1 - \frac{r^2}{2\bar{\sigma}_x^2}, \quad (12)$$

where $r = \sqrt{2k_u k_r \rho (x^2 + y^2)}$ is the scaled radial coordinate, $\bar{\sigma}_x = \sigma_x \sqrt{2k_u k_r \rho}$ is the scaled rms beam size, and $\bar{\sigma}_x^2 \gg 1$ is assumed for the last approximation. Let us separate the radiation profile in radial and azimuthal coordinates as

$$A(\bar{\mathbf{x}}) = B(r) e^{im\phi}. \quad (13)$$

Note that we suppress the explicit \bar{z} -dependence in Eq. (13) since $A(\bar{\mathbf{x}})$ depends on \bar{z} through the changing frequency detune in Eq. (11), which now becomes

$$\begin{aligned} \left[\mu_0 - \hat{\nu} + \frac{1}{2r} \frac{d}{dr} \left(r \frac{d}{dr} \right) - \frac{m^2}{2r^2} \right] B(r) \\ = \frac{1}{\mu_0^2} B(r) \left(1 - \frac{r^2}{2\bar{\sigma}_x^2} \right). \end{aligned} \quad (14)$$

The exact solution for this differential equation is

$$B(r) = \exp \left(\frac{-ir^2}{2\mu_0 \bar{\sigma}_x} \right) r^m L_n^m \left(\frac{ir^2}{\mu_0 \bar{\sigma}_x} \right), \quad (15)$$

where L_n^m is the associated Laguerre polynomial, and

$$n = \frac{1}{2} \left(-1 - m + \frac{i\bar{\sigma}_x}{\mu_0} - i\mu_0^2 \bar{\sigma}_x + i\mu_0 \nu \bar{\sigma}_x \right) \quad (16)$$

must be an integer so that $B(r)$ is bounded in r . This condition yields the dispersion relation

$$\mu_0 - \hat{\nu} - i \frac{(1 + m + 2n)}{\bar{\sigma}_x \mu_0} - \frac{1}{\mu_0^2} = 0. \quad (17)$$

Equations (15) and (17) are the generalization of Ref. [7] with azimuthal modes. In the limit when $\bar{\sigma}_x \gg 1$ (or $\sigma_x \gg 1/\sqrt{2k_1 k_u \rho}$), we can drop the $1/\bar{\sigma}_x$ term and arrive at the familiar 1D dispersion relation (see, e.g., Ref. [5]).

Fundamental Mode

For the fundamental mode with $n = m = 0$, we can denote

$$w = i\bar{\sigma}_x/(2\mu_0) \quad (18)$$

and write the rms mode size and angular divergence as

$$\sigma_r = \frac{\sigma_x}{2} \left[w_r \left(1 + \frac{w_i^2}{w_r^2} \right) \right]^{-1/2} \quad (19)$$

$$\sigma_{r'} = \frac{\lambda_1}{2\pi\sigma_x} \left[w_r \left(1 + \frac{w_i^2}{w_r^2} \right) \right]^{1/2}. \quad (20)$$

In the limit when $\bar{\sigma}_x \gg 1$ and at the optimal detune $\hat{\nu} = 0$, $\mu_0 \approx (-1 + i\sqrt{3})/2$, we then have

$$\sigma_r = \frac{\sigma_x}{2\sqrt{\sqrt{2k_u k_1 \rho}/3\sigma_x}} = \sqrt{\sigma_x \sigma_D}, \quad (21)$$

where

$$\sigma_D = \sqrt{\frac{3}{32k_u k_1 \rho}} \approx \sqrt{\frac{\lambda_1}{4\pi}} L_G \quad (22)$$

is the diffraction beam size, and

$$L_G = \frac{\lambda_u}{4\pi\sqrt{3}\rho} \quad (23)$$

is the 1D power gain length. Since $\bar{\sigma}_x \gg 1$, we have $\sigma_x \gg \sigma_D$. Equation (21) indicates that $\sigma_r < \sigma_x$, which is required in order for the expansion in Eq. (12) to be valid. An expression similar to Eq. (12) was discussed in Ref. [8].

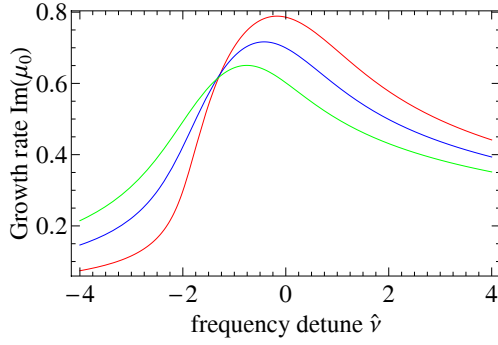


Figure 1: The growth rate μ_0 for the first three lowest-order modes: $m = n = 0$ (red); $m = 1$ and $n = 0$ (green); $m = 0$ and $n = 1$ (blue).

Higher-order Mode

For arbitrary n and m , the FEL mode is given by

$$A_{nm}(\bar{\mathbf{x}}) = r^m L_n^m \left(\frac{ir^2}{\mu_0 \bar{\sigma}_x} \right) \exp \left(-i \frac{r^2}{2\mu_0 \bar{\sigma}_x} + im\phi \right). \quad (24)$$

For example, we consider the case of the LCLS hard x-ray FEL at $\lambda_r = 1.5 \text{ \AA}$. For a 13.6 GeV beam with a normalized slice emittance $0.4 \mu\text{m}$, an average beta function 30 m in the undulator, we have $\sigma_x = 21 \mu\text{m}$. For $\rho = 5.8 \times 10^{-4}$ and $\lambda_u = 3 \text{ cm}$, we have $\bar{\sigma}_x \approx 2.1$. In Fig. 1, we show the zeroth-order growth rates of the first three lowest modes calculated from Eq. (17). We emphasize that this solution does not include the emittance and local energy spread effects, which are reasonably small for the high-brightness beam generated by the LCLS accelerator.

We note that when the frequency detune $\hat{\nu} < -1.5$ (when the FEL wavelength is longer than the resonant wavelength), higher-order modes can have higher growth rate than the fundamental mode. Such higher-order modes have larger angular divergence than the fundamental mode, which in turn shift the resonant wavelength towards the FEL wavelength and results in more efficient interactions with the electron beam.

TRANSVERSE EFFECTS OF FREQUENCY CHIRPED FELS

We now study the transverse effects of a SASE FEL introduced by frequency chirp (as well as undulator taper). Unlike a seeded FEL that has a well-defined frequency, a SASE FEL will determine its frequency spectrum through the gain process. Following the analysis of Ref. [4] (i.e., Eq. (44)), we find the central frequency of the SASE spectrum moves half as fast as does the optimal frequency (for maximum zeroth-order growth rate) due to the changing resonant condition, i.e., $\bar{\nu}_c = h\bar{z}/2$. Thus, we may write the frequency detune in Eq. (11) as

$$\hat{\nu} = \bar{\nu} - h\bar{z} = \bar{\nu} - \bar{\nu}_c - \frac{h\bar{z}}{2} = \Delta\bar{\nu} - \frac{h\bar{z}}{2}, \quad (25)$$

where $\Delta\bar{\nu} = \bar{\nu} - \bar{\nu}_c$. Thus, the effective frequency detune from the central frequency of a chirped SASE FEL is $-h\bar{z}/2$. We can also assume a (normalized) SASE spectrum as

$$P(\Delta\bar{\nu}) = \frac{1}{\sqrt{2\pi}\sigma_{\bar{\nu}}} \exp \left[-\frac{(\Delta\bar{\nu})^2}{2\sigma_{\bar{\nu}}^2} \right]. \quad (26)$$

The FEL saturation typically occurs when $z \approx \lambda_u/\rho$ or $\bar{z} \approx 4\pi$. At saturation we also have $\sigma_{\bar{\nu}} \approx 0.5$ or $\sigma_{\nu} \approx \rho$.

Near the FEL saturation, the fundamental mode usually dominates over the higher-order modes. To study the effects of frequency chirp on the transverse mode and coherence properties, we neglect the higher-order modes and take

$$A(\mathbf{x}) \approx \exp \left(-w \frac{\bar{\mathbf{x}}^2}{\bar{\sigma}_x^2} \right) = \exp \left(-w \frac{\mathbf{x}^2}{\sigma_x^2} \right). \quad (27)$$

We introduce the Wigner function for the transverse phase space of the radiation beam [9]

$$\begin{aligned} \Phi(\mathbf{x}, \mathbf{p}) &= \int d\mathbf{y} A \left(\mathbf{x} + \frac{\mathbf{y}}{2} \right) A^* \left(\mathbf{x} - \frac{\mathbf{y}}{2} \right) e^{ik_r \mathbf{p} \cdot \mathbf{y}} \\ &= \exp \left[-\frac{1}{2\beta\epsilon_r} (\alpha\mathbf{x} + \beta\mathbf{p})^2 \right], \end{aligned} \quad (28)$$

where

$$\alpha = \frac{w_i}{w_r}, \quad \beta = \frac{k_r \sigma_x^2}{2w_r}, \quad \epsilon_r = \frac{1}{2k_r} = \frac{\lambda_r}{4\pi}. \quad (29)$$

Here we use the analogous Twiss parameters to describe the transverse phase space of the FEL beam, and ϵ_r is the so-called diffraction-limited radiation emittance. Both α and β have strong dependence on the frequency detune. Hence the phase space ellipse for each frequency component has a slightly different orientation. For a SASE FEL with a finite bandwidth, the smearing of the transverse phase space ellipses contributes to a larger overall emittance than the diffraction-limited emittance ϵ_r and degrade the transverse coherence [10, 11]. To quantify this effect, we compute the second moment projected in the x direction at the FEL saturation when $\bar{z} = 4\pi$:

$$\begin{aligned} \langle x^2 \rangle &= \int d\bar{\nu} \epsilon_r \beta P(\Delta\bar{\nu}) = \int d\hat{\nu} \epsilon_r \beta P(\hat{\nu} + 2\pi h), \\ \langle xp_x \rangle &= - \int d\bar{\nu} \epsilon_r \alpha P(\Delta\bar{\nu}) = - \int d\hat{\nu} \epsilon_r \alpha P(\hat{\nu} + 2\pi h), \\ \langle p_x^2 \rangle &= \int d\bar{\nu} \epsilon_r \frac{1 + \alpha^2}{\beta} P(\Delta\bar{\nu}) \\ &= \int d\hat{\nu} \epsilon_r \frac{1 + \alpha^2}{\beta} P(\hat{\nu} + 2\pi h), \end{aligned} \quad (30)$$

and define the effective emittance for the radiation beam as

$$\epsilon_r^{\text{eff}} = \sqrt{\langle x^2 \rangle \langle p_x^2 \rangle - \langle xp_x \rangle^2}. \quad (31)$$

Similar expressions exist in the y direction. Note that both the angular divergence and the effective emittance are functions of the chirp parameter h . To calculate the degree

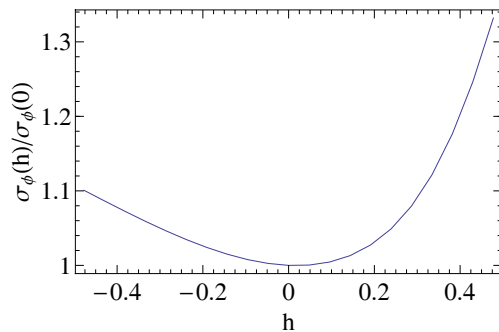


Figure 2: Angular divergence of the fundamental mode vs. frequency chirp.

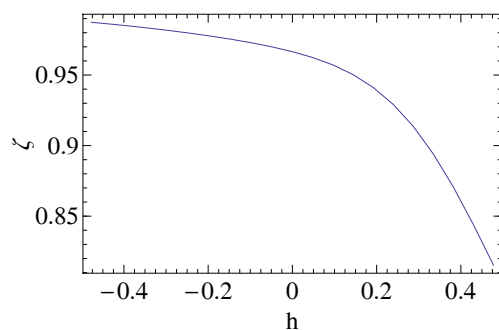


Figure 3: Degree of transverse coherence vs. frequency chirp.

of transverse coherence, we take the ratio of diffraction-limited emittance and the effective emittance in both x and y directions as

$$\zeta = \left(\frac{\epsilon_r}{\epsilon_r^{\text{eff}}} \right)^2. \quad (32)$$

To illustrate the above analysis, we consider again the case of the LCLS hard x-ray FEL at $\lambda_r = 1.5 \text{ \AA}$ and $\bar{\sigma}_x = 2.1$. Defining the average rms divergence of the radiation beam as $\sigma_\phi = (\langle p_x^2 \rangle)^{1/2}$ and using Eq. (30), we calculate the ratio $\sigma_\phi(h)/\sigma_\phi(0)$ as a function of the frequency chirp h in Fig. 2. We see that the angular divergence increases with increasing chirp amplitude. In Fig. 3, we show the degree of transverse coherence as computed from Eq. (32). We note that the transverse coherence decreases for a positive chirp but increases for a negative chirp. These effects have been observed in simulations as well.

DISCUSSIONS

As discussed in Ref. [2] for frequency chirp and Ref. [4] for undulator taper, slightly positive chirp and taper can enhance the FEL gain and increase the saturation power by a factor of ~ 2 . Through this 3D analysis, we show that positive chirp and taper decrease the transverse coherence while increase the angular divergence of such FELs.

We note that a small scaled chirp parameter h can mean a large relative chirp for the whole bunch. For example, $h = 0.1$ for the LCLS hard x-ray FEL means $\sim 6\%$ energy chirp over 70 fs bunch duration. However, if the bunch develops energy modulations through microbunching instability, then the local chirp can easily reach or exceed this value (i.e., $h = 0.1$ corresponds to an energy modulation amplitude $\sim 5 \times 10^{-4}$ for 1- μm modulation period).

Finally, for a bunch with a large positive chirp (i.e., head has a higher energy), the effective frequency detune is negative so that a higher-order mode may become dominant over the fundamental mode in a certain parameter regime, as illustrated in Fig. 1. The positive energy chirp can be created by off-crest rf acceleration or by longitudinal space charge, CSR and linac wakefield of a high-brightness beam. We note that the higher-order mode lasing was previously observed in the VISA FEL experiment [12].

ACKNOWLEDGEMENTS

We thank M. Yurkov for useful discussions. This work was supported by Department of Energy Contract No. DE-AC02-76SF00515.

References

- [1] S. Krinsky and Z. Huang, Phys. Rev. ST Accel. Beams **6**, 050702 (2003).
- [2] E.L. Saldin, E.A. Schneidmiller, and M.V. Yurkov, Phys. Rev. ST Accel. Beams **9**, 050702 (2006).
- [3] J. Wu *et al.*, J. Opt. Soc. Am. B **24**, 484 (2007).
- [4] Z. Huang, G. Stupakov, Phys. Rev. ST Accel. Beams **8**, 040702 (2005).
- [5] R. Bonifacio, C. Pellegrini, and L. M. Narducci, Opt. Commun. **50**, 373 (1984).
- [6] M. Xie, Nucl. Instrum. Methods A **445**, 59 (2000).
- [7] M. Xie, Ph.D. dissertation, Stanford University (1988).
- [8] Z. Huang and K.-J. Kim, Phys. Rev. ST Accel. Beams **10**, 034801 (2007).
- [9] K.-J. Kim, AIP Conference Proceedings **367**, 565 (AIP, New York, 1989).
- [10] E.L. Saldin, E.A. Schneidmiller and M.V. Yurkov, Opt. Commun. **186**, 185 (2000).
- [11] K.-J. Kim and Z. Huang, AIP Conference Proceedings **581**, 185 (AIP, New York, 2001).
- [12] A. Murokh *et al.*, Phys. Rev. E **67**, 066501 (2003).